

SPIDER: a Balloon-borne Large-scale CMB Polarimeter

B. P. Crill^{a,b}, P.A.R. Ade^c, E. S. Battistelli^d, S. Benton^e, R. Bihary^f, J. J. Bock^{g,h}, J. R. Bond^b, J. Brevik^h, S. Bryan^f, C. R. Contaldiⁱ, O. Doré^b, M. Farhang^a, L. Fissel^a, S. R. Golwala^h, M. Halpern^c, G. Hilton^j, W. Holmes^g, V. V. Hristov^h, K. Irwin^j, W. C. Jones^{g,h}, C. L. Kuo^k, A. E. Lange^h, C. Lawrie^f, C. J. MacTavish^b, T. G. Martin^l, P. Mason^h, T. E. Montroy^f, C. B. Netterfield^{a,e}, E. Pascale^c, D. Riley^f, J. E. Ruhl^f, M. C. Runyan^h, A. Trangsrud^h, C. Tucker^c, A. Turner^g, M. Viero^a, and D. Wiebe^e.

^aDepartment of Astronomy and Astrophysics, University of Toronto, Toronto, ON, Canada;

^bCanadian Institute for Theoretical Astrophysics (CITA), University of Toronto, ON, Canada;

^cSchool of Physics and Astronomy, Cardiff University, UK;

^dDepartment of Physics and Astronomy, University of British Columbia, Vancouver, BC, Canada;

^eDepartment of Physics, University of Toronto, ON, Canada;

^fDepartment of Physics, Case Western Reserve University, Cleveland, OH, USA;

^gJet Propulsion Laboratory, Pasadena, CA, USA;

^hDepartment of Physics, California Institute of Technology, Pasadena, CA, USA;

ⁱTheoretical Physics, Blackett Laboratory, Imperial College, London, UK;

^jNational Institute of Standards and Technology, Boulder, CO, USA;

^kDepartment of Physics, Stanford University, Palo Alto, CA, USA;

^lDepartment of Mechanical and Industrial Engineering, University of Toronto, ON, Canada

ABSTRACT

SPIDER is a balloon-borne experiment that will measure the polarization of the Cosmic Microwave Background over a large fraction of a sky at $\sim 1^\circ$ resolution. Six monochromatic refracting millimeter-wave telescopes with large arrays of antenna-coupled transition-edge superconducting bolometers will provide system sensitivities of 4.2 and 3.1 $\mu\text{K}_{\text{cmb}}\sqrt{\text{s}}$ at 100 and 150 GHz, respectively. A rotating half-wave plate will modulate the polarization sensitivity of each telescope, controlling systematics. Bolometer arrays operating at 225 GHz and 275 GHz will allow removal of polarized galactic foregrounds. In a 2-6 day first flight from Alice Springs, Australia in 2010, SPIDER will map 50% of the sky to a depth necessary to improve our knowledge of the reionization optical depth by a large factor.

1. INTRODUCTION

Rapid progress in millimeter-wave receiver technology enabled major advances in cosmology over the past decade. Extremely sensitive receivers measured the very faint anisotropies and polarization of the Cosmic Microwave Background (CMB), which are a mere part in 10^5 and 10^6 of the background, respectively. CMB observations from the ground, stratospheric balloons, and space have confirmed and powerfully constrained the standard model of cosmology. Two periods of the history of the universe still elude complete description: the period of inflation in the very early universe, and the period of first star formation that reionized the intergalactic medium in the more recent universe.

The theory of inflation postulates a period of very rapid expansion of the Universe ($\sim 10^{-36}$ seconds after the Big Bang) that seeded the formation of structure. The theory remains incomplete and current observations only provide general constraints.¹ Inflation also predicts that the universe is filled with gravitational waves generated

Further author information: (Send correspondence to B.P.Crill) E-mail: crill@astro.utoronto.ca, Telephone: +1 416 978 0307

in the early universe. The gravitational waves have extremely long wavelength, making them difficult to detect directly, but they leave a unique imprint in the polarization pattern in the CMB: the B-mode polarization. Measuring the B-mode signal (a part in 10^7 of the background) requires another leap forward in technology.

The CMB also provides a way to investigate the period of reionization of the universe. Reionization enhances polarization and anisotropies on scales larger than the horizon size at reionization and damps them on smaller scales. Measuring the scale of damping and the amount tells us the optical depth of reionized universe through which the CMB photons have travelled. Finding the signature of reionization is easiest in polarization, as other cosmological parameters can create a similar signature in the temperature anisotropy. The 5 year results from WMAP included a measurement of the total integrated optical depth, but tighter constraints could be found with a more sensitive instrument.

Here we describe SPIDER, a balloon-borne instrument designed to measure the polarization of the CMB over a large fraction of the sky at large angular scales. The optical design of SPIDER, including a rotating half-wave plate at the telescope aperture and on-axis monochromatic refracting telescopes, will provide the required control of systematics. Large arrays of antenna-coupled transition-edge superconducting bolometers with multiplexed SQUID readouts provide the raw sensitivity for probing inflation and reionization. The choice of frequency bands in SPIDER will minimize confusion from galactic foregrounds. SPIDER complements *Planck* with its greater control of polarization systematics and closely spaced passbands for polarized foreground characterization.

The instrument will make a 2-6 day first flight from Alice Springs, Australia in the austral autumn of 2010 that will probe the reionization of the universe with an unprecedented measurement of the large scale polarization of the CMB. Subsequent flights will provide the longer integration time necessary for investigating inflation. The balloon-borne platform is an ideal environment for these observations, allowing observation of nearly half the sky.

The SPIDER instrument was introduced in Montroy et al. (2006).² MacTavish et al. (2007)³ made a detailed investigation of systematics in SPIDER observations. Here we discuss modifications in the instrument design and discuss the prospects for scientific results from our first flight.

2. SCIENCE GOALS

Polarization of the CMB comes from Thomson scattering of anisotropic radiation by electrons in the primordial plasma at the surface of last scattering, when the CMB was emitted. No circular polarization is created by this process. The linear polarization pattern on the full sky can be decomposed into rotationally invariant E-modes and B-modes. These quantities are linearly related to the Stokes parameters Q and U*. The majority of the polarized signal in the CMB is due to the velocity of the primordial plasma and appears as a series of acoustic peaks in the E-mode angular power spectrum. Cosmological B-mode polarization is uniquely produced by very long wavelength gravitational waves generated the early universe (see Section 2.3 below).

SPIDER's first flight will be a turnaround flight[†] from Alice Springs, Australia, of 2-6 days duration in the austral autumn of 2010. While the sun is below the horizon, SPIDER will operate in its spinning mode, and will map $\sim 50\%$ of the sky each night. When the sun is between the horizon and 45° elevation, SPIDER will scan a reduced section of the sky in the anti-sun direction. During this initial flight, SPIDER will make measurements of the large scale E-mode angular power spectrum of the CMB and dust polarization at large angular scales.

Future flights of SPIDER will be Long Duration Balloon flights of 20-30 days from Antarctica or from Alice Springs and will provide the long integration time necessary to target the the signature of primordial gravitational waves in the B-mode power spectrum.

*Q and U completely describe the polarization of the CMB, but are coordinate-dependent quantities.

[†] *Turnaround* refers to a balloon launched at the time of the seasonal reversal of the stratospheric wind direction; the balloon drifts slower in longitude.

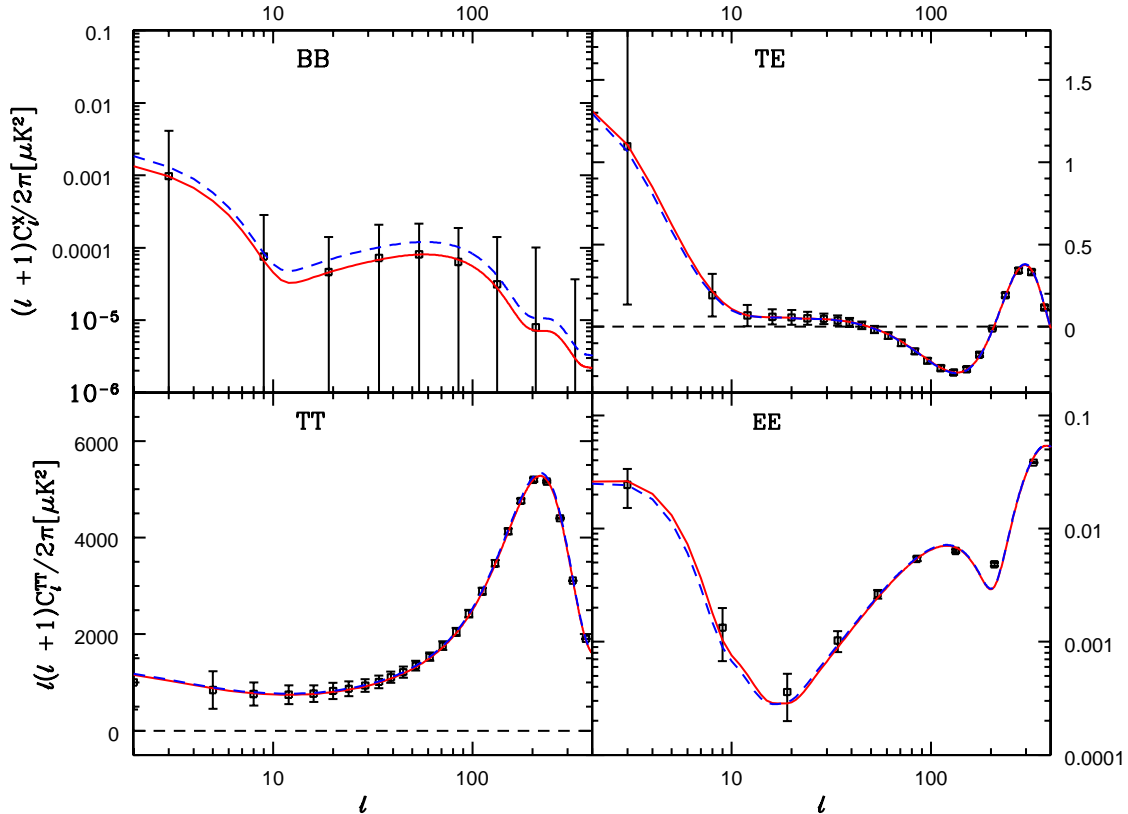


Figure 1. Simulated recovery of the temperature and polarization angular power spectra from a 4-day first flight of SPIDER, with 100 and 145 GHz as in Table 1. The simulations of time-ordered data include $1/f$ noise with a 100 mHz knee frequency. The half-wave plate is stepped each hour during the daytime scan mode and each night during nighttime spin mode. The sky signal is reconstructed from the time ordered data with a naively binned map-maker, power spectra are estimated with *xfaster*.⁴ The input model (solid curve) is the best fit Λ CDM + tensors of WMAP3. The dashed curve is our own best fit spectrum with *cosmomc* software⁵ - see Figure 2. These are expected to be conservative estimates of SPIDER’s sensitivity; we expect to reduce the error in the lowest EE bin by $\sim 30\%$ with an optimal map maker.

2.1 The Epoch of Reionization

A variety of astrophysical measurements show that the Universe was ionized sometime before redshift of $z \sim 6$,^{6,7} presumably due to ultraviolet photons from star formation. Measurement of the large-scale polarization of the CMB provides a very sensitive measurement of the total optical depth of the reionized universe out to the surface of last scattering. The five-year observations of WMAP give an optical depth of $\tau = 0.087 \pm 0.017$. Assuming that reionization occurred instantaneously, it occurred at a redshift 11.0 ± 1.4 .⁸ A deeper polarization map from SPIDER’s test flight will give a measurement of the optical depth that is many times more precise than WMAP’s 5-year measurement (Figure 2). The improvement comes from SPIDER’s deep measurement of polarization on the largest scales, a unique measurement from a suborbital mission.

2.2 Dust in the Galaxy

The polarized signal from the galaxy at millimeter wavelengths is mainly from synchrotron at frequencies below 70 GHz and thermal emission by dust at higher frequency. WMAP provides measurements of synchrotron emission⁹ and in doing so, make a map of the large scale magnetic field of the galaxy.¹⁰ Dust grains preferentially align along galactic magnetic fields, polarizing the thermal emission. SPIDER’s frequency coverage is chosen to distinguish CMB polarization from dust,² making SPIDER an ideal instrument for dust studies. The degree of

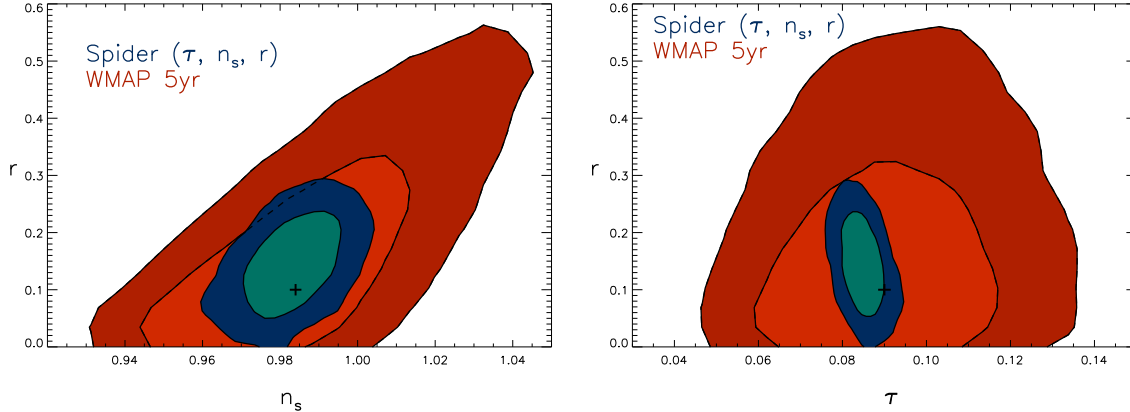


Figure 2. Marginalized likelihood contours for WMAP 5-year and SPIDER’s first flight. r is the ratio of tensor perturbations to scalar perturbations, τ is the optical depth through reionization, and n_s is the spectral index of scalar perturbations. The $+$ represents the input value of the parameters; in this case $n_s = 0.984$, $r = 0.1$, $\tau = 0.09$. SPIDER’s improvement comes from more sensitive polarimetry on large scales.

grain alignment (and hence polarization fraction in the SPIDER passbands) depends on the physical properties of the dust grains. Additionally, using polarized dust emission to constrain the magnetic field strength on smaller scales in the galaxy gives insight into the role of magnetic fields in star formation.

2.3 Probing Inflation

A third science goal of SPIDER is to probe the energy scale of the inflationary period of the Universe by mapping the polarization of the CMB on very large scales.

Inflation is a postulated period of exponential expansion of the early universe, caused by an inflaton field with negative pressure. Inflation solves problems in the standard model of cosmology, such as the horizon problem and the flatness problem, but the theory is most compelling as a means of seeding structure formation. Quantum perturbations in the inflaton field expanded to cosmological sizes during inflation. These inhomogeneities in the inflaton field drove density perturbations in matter and radiation, which in turn produced anisotropies in the CMB and eventually structure in the Universe. The existence of acoustic peaks in the CMB anisotropy spectrum give circumstantial evidence to the inflationary scenario of structure formation.¹¹

The imprint of gravitational waves on the CMB provides a direct way to probe inflation. Inflation produces perturbations in the metric tensor, effectively a background of super-horizon gravitational waves, that do not lead to structure formation, but do leave an imprint on the anisotropy and polarization of the CMB. The gravitational wave background is the only cosmological means of generating B-mode fluctuations, and as such, is a unique signature of inflation.

The amplitude of the gravitational waves is parametrized with the tensor-to-scalar ratio r , the ratio of power in primordial tensor perturbations to power in scalar perturbations. The amplitude of the gravitational waves is directly proportional to the energy scale of the inflaton particle before inflation. In turn, the amplitude of the B-modes directly measures the energy scale of inflation. The tightest limit on r is from WMAP; assuming a power-law for the spectrum of tensor and scalar fluctuations, $r < 0.43$.⁸ A long duration flight of SPIDER has excellent prospects of measuring the B-mode signal;² however, SPIDER’s first flight will not have long enough integration time to do so.

3. INSTRUMENT

The SPIDER payload is shown in Figure 3. The pointing and pointing reconstruction systems build on experience from the BOOMERANG¹² and BLAST¹³ designs. The payload observes two ways: scanning in azimuth or spinning. The inner frame is adjustable in elevation with a simple linear actuator similar to the BOOMERANG design.

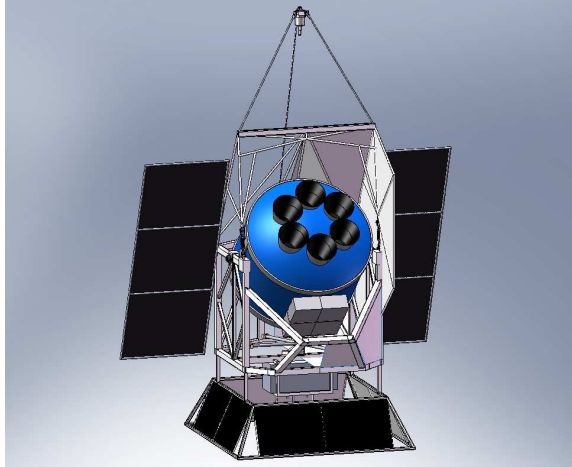


Figure 3. The SPIDER payload. Six independent monochromatic telescopes are housed in a single long hold time cryostat. Each telescope is fully baffled from radiation from the ground and balloon. The gondola scans in azimuth with a reaction wheel and a motorized pivot. The cryostat, mounted on bearings, can be adjusted in elevation. Solar arrays provide power.

Multiple tracking star cameras, rate gyros, differential GPS and a sun sensor provide pointing information. The gondola is constructed from carbon fibre tubes to save mass.

4. CRYOGENICS

The cryostat for the SPIDER instrument uses liquid helium-4 (LHe) to cool the instrument during its flight. All six instrument inserts and the ~ 1000 litre LHe tank are contained in an outer vacuum vessel fabricated by Redstone Aerospace. The primary LHe tank is maintained at 108 kPa and a small (~ 20 litre) capillary-fed superfluid LHe tank will be controlled at a vapour pressure near 100 Pa. The inserts and the liquid cryogen tanks are surrounded by two concentric vapour-cooled shields and the inner tank is mechanically supported by G10 flextures. The use of staged vapour-cooled shields and radiation blockers reduces the radiative loading on the optics and detectors. Closed-cycle ^3He sorption refrigerators, one per focal plane, will cool the detectors to 260 mK from the 1.5K base temperature. The sorption fridges are cycled every 48 hours.

5. OPTICAL DESIGN

5.1 Telescope

The optical design is based on the successful *Robinson/BICEP* telescope.¹⁴ Each telescope is a monochromatic, telecentric refractor with anti-reflection-coated polyethylene lenses, and is cooled to 4K. The aperture field distribution of the primary is smoothly tapered with an anodized 4K Lyot stop, reducing the detector background.

5.2 Half-wave Plate

SPIDER modulates the polarization of the incoming light with a stepped half-wave plate (HWP) at the telescope aperture. Modulating the polarization mitigates systematic errors from asymmetric beams, instrumental polarization and relative gain uncertainty between detectors.

A HWP placed at the aperture of the telescope rotates the angle of polarization sensitivity on the sky at four times the physical rotation rate of the HWP, while leaving the beams unchanged. It also enables a full measurement of the sky polarization using each individual detector, eliminating or reducing many potential systematic effects.

SPIDER's single-frequency telescopes simplify the HWP design and implementation. A single birefringent sapphire wave plate coated with a single layer of fused quartz on each side gives very good (band average of

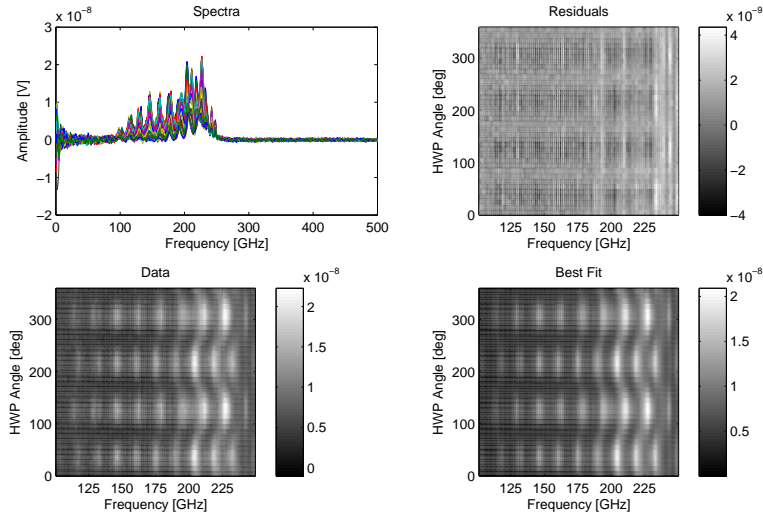


Figure 4. Measurements of the transmission of a polarized signal as a function of frequency and rotation angle for a single birefringent sapphire plate appropriate for our 150GHz band, which will be used in SPIDER’s half-wave plate with an anti-reflection (AR) coating. The data are well-described by a birefringence model that gives an index difference of $\Delta n = 0.3350 \pm 0.0003$ between the fast and slow axes. The model fit also recovers the angle of the crystal axes to 0.1° precision. The addition of an AR-coat greatly reduces the channel spectra evident in band.

96.8% modulation efficiency) performance over a 25% bandwidth. Measurements of a prototype HWP with no anti-reflection coating (Figure 4) show excellent polarization modulation across the SPIDER band.

6. DETECTORS AND READOUT

6.1 Detectors and SQUIDS

SPIDER uses a large-format array of antenna-coupled bolometers,¹⁵ shown in Figure 5. Each spatial pixel consists of a 16×16 phased array of slot dipole antennae. The pixel’s radiation pattern is defined by the coherent interference of the antenna elements, yielding a $\sim 13^\circ$ FWHM beam with a first sidelobe at -15 dB when the 256 elements are fed with equal weights. Each spatial pixel has two orthogonally polarized antennae.[‡] With the radiation pattern of the antenna array terminated on the 4K stop, the system produces highly symmetrical beams on the sky with low cross-polarization. The optical power is transmitted via superconducting microstrip¹⁶ to superconducting transition-edge sensors (TESs).¹⁷

The array design has a bandwidth of close to 30%, set by the slot length. Optical band definition is provided by a combination of in-line microstrip filters and cryogenic metal-mesh optical filters, the combination of which provide sharp band edges and no intrinsic out-of-band response (see Figure 5).

The TESs have strong electro-thermal feedback and low heat capacity, providing an extremely linear and fast bolometer.^{18–20} Thermal isolation of the TES films is provided by Si_3N_4 support legs. Optical power is deposited in the TES by terminating the superconducting microstrip with a long gold meander on the same thermal island as the TES.

The antenna-coupled design is entirely photolithographically fabricated, greatly simplifying production and the uniformity of large-format arrays. The integrated components are mechanically robust, and immune to differential thermal contraction. The densely populated antennae allow a very efficient use of the focal plane area. The antenna-coupled architecture has been successfully demonstrated.^{17,21} We have thoroughly characterized a

[‡]Each detector will be able to measure Q and U independently, but this is due to the use of a HWP and scan strategy to modulate the angle of polarization sensitivity. The dual polarization design of the pixels is primarily useful for high device packing density.

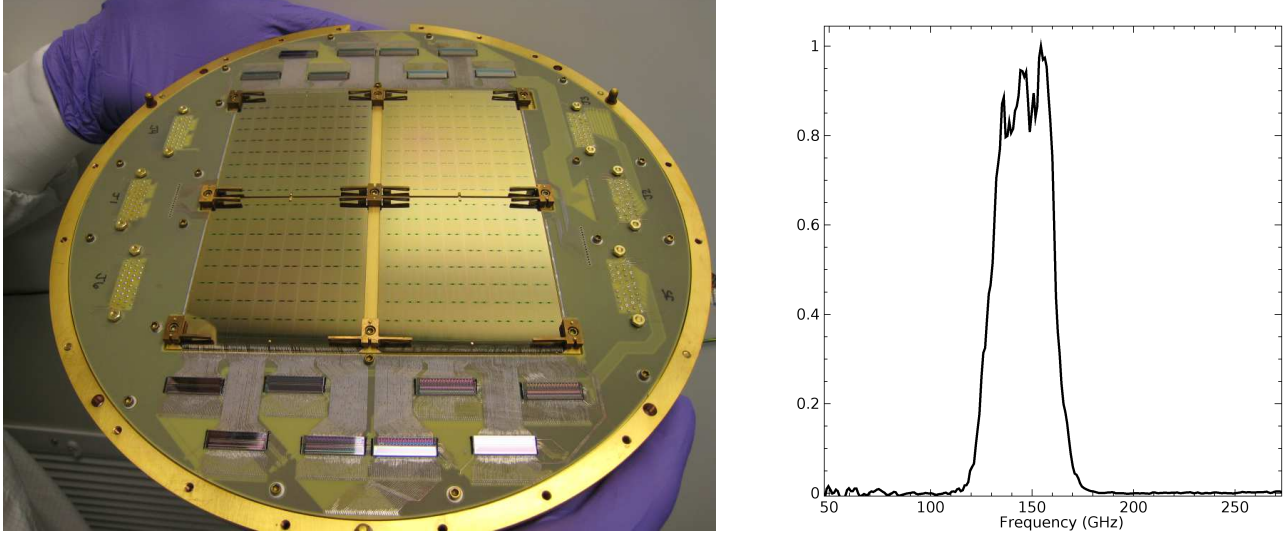


Figure 5. Left: A prototype SPIDER focal plane unit, consisting of four detector wafers. Each wafer comprises 64 spatial pixels, sensing two polarizations each, and read out by 128 detectors. The smaller chips on the periphery are NIST column multiplexer chips, each reading out 32 detectors. Light enters through a square aperture under the tiles, back illuminating the detectors. A niobium plate covers the entire assembly and serves as a superconducting magnetic shield as well as a backshort surface for the antennae. Right: the passband of a 145 GHz device. This passband is of the device alone, the SPIDER optical train is not yet mated to the detector.

Band Centre (GHz)	Bandwidth (GHz)	Beam FWHM (arcmin)	Number of Spatial Pixels	Number of Detectors	Single-Detector Sensitivity ($\mu\text{K}_{\text{CMB}}\sqrt{\text{s}}$)	Instrument Sensitivity ($\mu\text{K}_{\text{CMB}}\sqrt{\text{s}}$)
100	24	58	(2×)144	(2×)288	100	4.2
145	35	40	(2×) 256	(2×) 512	100	3.1
225	54	26	256	512	204	9.0
275	66	21	256	512	351	15.5

Table 1. Observing bands, pixel and detector counts, and single-detector and instrument sensitivities. The latter is obtained by dividing the single-detector sensitivity by $\sqrt{N_{\text{det}}}$. A total of 2624 detectors are distributed between the six telescopes, with two telescopes in each of the 100 GHz and 145 GHz bands.

series of end-to-end prototype detectors at 96 and 150 GHz. Radiation patterns, measured with both optically modulated thermal sources and monochromatic sources, confirm the theoretical predictions. The inline filters show well defined bands with $\sim 30\%$ bandwidth.

The distribution of the pixels and the per-pixel sensitivities are indicated in Table 1. In the CMB science bands (100 and 150 GHz), sensitivities are dominated by photon and phonon noises which contribute roughly equally. Johnson and amplifier noises are negligible.

The TES sensors will be read out using superconducting quantum interference device (SQUID) current amplifiers with time-domain multiplexing. Ambient temperature multi-channel electronics (MCE)²² which work in concert with time-domain multiplexers.^{23–26} The MCE were initially developed for SCUBA2²⁷ and are used as read-out electronics on many CMB and sub-mm astronomy receivers (e.g. ACT,²⁸ C_ℓOVER,²⁹ BICEP II and SPUD³⁰).

6.2 Magnetic Shielding

Magnetic shielding is a critical requirement for SPIDER’s receiver. We use a combination of high-permeability and superconducting shields to achieve the necessary reduction in magnetic field. A SQUID amplifier measures current via the magnetic flux in its input inductor coil, therefore it also responds to variations in the ambient

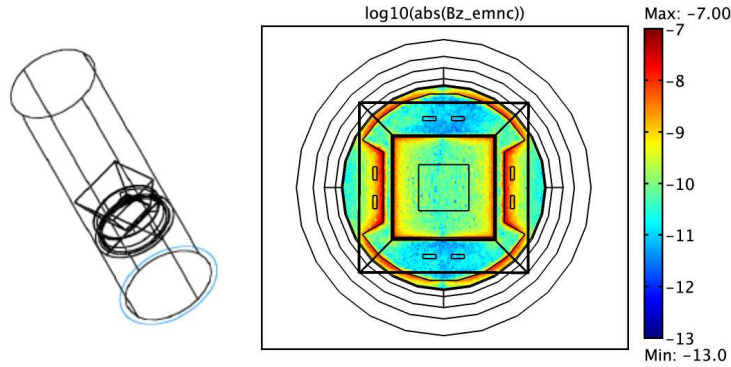


Figure 6. *Left:* Magnetic shielding design for SPIDER. The SPIDER design incorporates a single layer of cryoperm at 4K (long tube, 1.25m long), a sub-K superconducting box with a flared opening through which light enters, and a superconducting plane just under the array. *Right:* the z-component of the magnetic field in the focal plane, 500 μm above the superconducting plane. A 50 μT field has been applied at a 45° angle to the optical axis. The hourglass shape is the outline of the superconducting plane – the vertical field is highest at the edges where it goes around the superconducting plane. The large square in the centre represents the TES focal plane. The rectangles at the top and bottom of the plot are indicative of where the SQUIDs will be placed. We find a residual field of $< 300\text{pT}$ over most of the TES focal plane and at the few pT level at the SQUIDs.

Desired Depth	0.5 μK_{CMB}
Ambient Field	50 μT
TES G	20 pW/K
TES T_{bolo}/T_{CMB} responsivity	7 mK/K_{CMB}
TES field sensitivity	2.7 $\mu\text{K}_{CMB}/\text{nT}$
Residual field requirement	180 pT
Attenuation requirement	3×10^9

Desired Depth	0.5 μK_{CMB}
Ambient Field	50 μT
SQUID field/ TES current	0.5 pA/pT
TES current/ T_{CMB} responsivity	0.7 $\text{pA}/\mu\text{K}_{CMB}$
Field sensitivity via SQUID	0.7 $\mu\text{K}_{CMB}/\text{pT}$
Residual field requirement	0.7 pT
Attenuation requirement	7×10^7

Table 2. *Left:* Summary of TES magnetic field sensitivity and shielding requirements. We consider the 150 GHz band with optical efficiency 0.4 and a TES field sensitivity of $1\text{mK}/50\mu\text{T}$. *Right:* Summary of SQUID magnetic field sensitivity. The input coil / SQUID mutual inductance is 275pH.

magnetic field (albeit reduced by a quadrupole gradiometric input coil). Additionally, the critical temperature (T_c) of the TES devices depend on the applied field. These susceptibilities can be measured in the lab, allowing us to set a specification for the required level of magnetic shielding. Our requirement on spurious field signal is that it is less than the expected map rms on 1° pixels.

We distinguish between two types of sources of magnetic fields: 1) "ambient" fields over which we have no control; and 2) fields generated locally by motors and electronics on the instrument or in the nearby environment. A typical value of Earth's magnetic field $50\mu\text{T}$. The local magnetic field due to SPIDER's azimuth drive will be less than 1nT at the location of the focal plane. We therefore focus on shielding of the ambient field.

We have measured a $1\text{mK}/50\mu\text{T}$ field dependence of T_c for our Ti TES devices. Table 2 presents the ambient fields, field sensitivity, and resulting shielding requirements for SPIDER. In the case of the SQUID susceptibility, the parameter in question is "effective area", which converts from applied field to magnetic flux. The current NIST design has an effective area of $(12\mu\text{m})^2$. We show in Table 2 how this susceptibility feeds through the system. If insufficient, we also try, at some cost in complexity: a) using driven coils to null Earth's field or b) use AC modulation of the TES bias to move the science signal outside the field pickup band.

We have designed a magnetic shielding using COMSOL finite element calculations³¹ (see Figure 6); the residual field levels meet the TES and SQUID susceptibility goals listed in Table 2. Additional rejection of field signals based on the use of dark pixels or common-mode signals among many science pixels will provide a large safety margin over these estimates.

Systematic	Experimental Spec.	Comments
Receiver 1/f knee	< 200 mHz	for 110 degrees per second gondola spin
Receiver 1/f knee	< 100 mHz	for 36 degrees per second gondola spin
Pointing Jitter	< 10'	sufficient for $\ell < 50$
Absolute Pol. Angle Offset	< 0.25°	
Relative Pol. Angle Offset	< 1°	
Beam Centroid Positions	< 1'	sufficient for $\ell < 30$
Optical Ghosting	< 2%	% TOD contamination
Calibration Drift	< 3.0%	in phase
Calibration Drift	< 0.1%	out of phase

Table 3. Summary of experimental specifications based on simulation results, a reproduction of Table 2 of MacTavish et al (2007).. Realistic-amplitude, time-varying systematics are simulated in time streams. Maps are reconstructed without any attempt to correct for the systematic errors. Experimental specifications are set by limiting the allowed systematic residual level to a factor of ~ 10 smaller than the B-mode signal for $r = 0.01$. The nominal operating mode is a 36 dps gondola spin rate, with the half-wave plate stepping 22.5° once per day, with 10 iterations of a Jacobi iterative map-maker.³⁴ Each of these specifications is easily met by SPIDER.

7. FOREGROUNDS AND SYSTEMATICS

Polarized emission from the galaxy confuses measurements of CMB polarization, and is likely to set the ultimate limit on measurement of B-modes. The bandpasses for SPIDER are selected to distinguish E- and B-mode signals from galactic emissions. The band selection strategy has not changed since Montroy et al (2006) and we refer the reader to that work.²

Instrumental systematic effects present a huge challenge for the measurement of nanoKelvin polarization signals on the sky.^{32,33} MacTavish et al. (2007)³ investigate systematics in the specific case of SPIDER using a full data analysis pipeline. This set of simulations set specifications on instrumental design and on in-flight or pre-flight knowledge of various instrumental parameters (Table 3).

8. CONCLUSIONS

SPIDER is unique as a sub-orbital millimeter-wave polarimeter that can observe a large fraction of the sky. Large-format multiplexed TES bolometer arrays provide excellent raw sensitivity, and the refracting optical design and a rotating half-wave plate will minimize systematics. In its first flight, SPIDER will make a precise measurement of the optical depth of reionization. Later flights will measure the B-mode signal from primordial gravitational waves.

SPIDER acts a pathfinder to the proposed CMBpol space mission more than any other planned B-mode experiment. SPIDER will test a receiver with a large format array and multiplexed readout electronics in a high-altitude environment as well as observing strategies and systematics of deep polarimetry on a large fraction of the sky. The design of SPIDER emphasizes lightweighting, power savings, and autonomous operation all of which are directly applicable to a space mission.

ACKNOWLEDGMENTS

We acknowledge funding from NASA (grant number NNX07AL64G), the Gordon and Betty Moore Foundation, and NSERC. We are grateful to Danny Ball and the Columbia Scientific Ballooning Facility for assistance with flight planning.

REFERENCES

- [1] Komatsu, E., Dunkley, J., Nolta, M. R., Bennett, C. L., Gold, B., Hinshaw, G., Jarosik, N., Larson, D., Limon, M., Page, L., Spergel, D. N., Halpern, M., Hill, R. S., Kogut, A., Meyer, S. S., Tucker, G. S., Weiland, J. L., Wollack, E., and Wright, E. L., “Five-Year Wilkinson Microwave Anisotropy Probe (WMAP) Observations: Cosmological Interpretation,” *ArXiv e-prints* **803** (Mar. 2008).

- [2] Montroy, T. E., Ade, P. A. R., Bihary, R., Bock, J. J., Bond, J. R., Brevick, J., Contaldi, C. R., Crill, B. P., Crites, A., Doré, O., Duband, L., Golwala, S. R., Halpern, M., Hilton, G., Holmes, W., Hristov, V. V., Irwin, K., Jones, W. C., Kuo, C. L., Lange, A. E., MacTavish, C. J., Mason, P., Mulder, J., Netterfield, C. B., Pascale, E., Ruhl, J. E., Trangsrud, A., Tucker, C., Turner, A., and Viero, M., “SPIDER: a new balloon-borne experiment to measure CMB polarization on large angular scales,” in [*Ground-based and Airborne Telescopes. Edited by Stepp, Larry M.. Proceedings of the SPIE, Volume 6267, pp. 62670R (2006).*], Presented at the Society of Photo-Optical Instrumentation Engineers (SPIE) Conference **6267** (July 2006).
- [3] MacTavish, C. J., Ade, P. A. R., Battistelli, E. S., Benton, S., Bihary, R., Bock, J. J., Bond, J. R., Brevik, J., Bryan, S., Contaldi, C. R., Crill, B. P., Doré, O., Fissel, L., Golwala, S. R., Halpern, M., Hilton, G., Holmes, W., Hristov, V. V., Irwin, K., Jones, W. C., Kuo, C. L., Lange, A. E., Lawrie, C., Martin, T. G., Mason, P., Montroy, T. E., Netterfield, C. B., Riley, D., Ruhl, J. E., Trangsrud, A., Tucker, C., Turner, A., Viero, M., and Wiebe, D., “Spider Optimization: Probing the Systematics of a Large Scale B-Mode Experiment,” *ArXiv e-prints* **710** (Oct. 2007).
- [4] Contaldi, C. and et al. in preparation (2008).
- [5] Lewis, A. and Bridle, S., “Cosmological parameters from CMB and other data: A Monte Carlo approach,” *Phys. Rev. D* **66**, 103511–+ (Nov. 2002).
- [6] Malhotra, S. and Rhoads, J. E., “Luminosity Functions of Ly α Emitters at Redshifts $z=6.5$ and $z=5.7$: Evidence against Reionization at $z\leq 6.5$,” *ApJ* **617**, L5–L8 (Dec. 2004).
- [7] Totani, T., Kawai, N., Kosugi, G., Aoki, K., Yamada, T., Iye, M., Ohta, K., and Hattori, T., “Implications for Cosmic Reionization from the Optical Afterglow Spectrum of the Gamma-Ray Burst 050904 at $z = 6.3$,” *PASJ* **58**, 485–498 (June 2006).
- [8] Dunkley, J., Komatsu, E., Nolta, M. R., Spergel, D. N., Larson, D., Hinshaw, G., Page, L., Bennett, C. L., Gold, B., Jarosik, N., Weiland, J. L., Halpern, M., Hill, R. S., Kogut, A., Limon, M., Meyer, S. S., Tucker, G. S., Wollack, E., and Wright, E. L., “Five-Year Wilkinson Microwave Anisotropy Probe (WMAP) Observations: Likelihoods and Parameters from the WMAP data,” *ArXiv e-prints* **803** (Mar. 2008).
- [9] Gold, B., Bennett, C. L., Hill, R. S., Hinshaw, G., Odegard, N., Page, L., Spergel, D. N., Weiland, J. L., Dunkley, J., Halpern, M., Jarosik, N., Kogut, A., Komatsu, E., Larson, D., Meyer, S. S., Nolta, M. R., Wollack, E., and Wright, E. L., “Five-Year Wilkinson Microwave Anisotropy Probe (WMAP) Observations: Galactic Foreground Emission,” *ArXiv e-prints* **803** (Mar. 2008).
- [10] Page, L., Hinshaw, G., Komatsu, E., Nolta, M. R., Spergel, D. N., Bennett, C. L., Barnes, C., Bean, R., Doré, O., Dunkley, J., Halpern, M., Hill, R. S., Jarosik, N., Kogut, A., Limon, M., Meyer, S. S., Odegard, N., Peiris, H. V., Tucker, G. S., Verde, L., Weiland, J. L., Wollack, E., and Wright, E. L., “Three-Year Wilkinson Microwave Anisotropy Probe (WMAP) Observations: Polarization Analysis,” *ApJS* **170**, 335–376 (June 2007).
- [11] Lange, A. E., Ade, P. A., Bock, J. J., Bond, J. R., Borrill, J., Boscaleri, A., Coble, K., Crill, B. P., de Bernardis, P., Farese, P., Ferreira, P., Ganga, K., Giacometti, M., Hivon, E., Hristov, V. V., Iacoangeli, A., Jaffe, A. H., Martinis, L., Masi, S., Mauskopf, P. D., Melchiorri, A., Montroy, T., Netterfield, C. B., Pascale, E., Piacentini, F., Pogosyan, D., Prunet, S., Rao, S., Romeo, G., Ruhl, J. E., Scaramuzzi, F., and Sforna, D., “Cosmological parameters from the first results of Boomerang,” *Phys. Rev. D* **63**, 042001–+ (Feb. 2001).
- [12] Masi, S., Ade, P. A. R., Bock, J. J., Bond, J. R., Borrill, J., Boscaleri, A., Cabella, P., Contaldi, C. R., Crill, B. P., de Bernardis, P., de Gasperis, G., de Oliveira-Costa, A., de Troia, G., di Stefano, G., Ehlers, P., Hivon, E., Hristov, V., Iacoangeli, A., Jaffe, A. H., Jones, W. C., Kisner, T. S., Lange, A. E., MacTavish, C. J., Marini Bettolo, C., Mason, P., Mauskopf, P. D., Montroy, T. E., Nati, F., Nati, L., Natoli, P., Netterfield, C. B., Pascale, E., Piacentini, F., Pogosyan, D., Polenta, G., Prunet, S., Ricciardi, S., Romeo, G., Ruhl, J. E., Santini, P., Tegmark, M., Torbet, E., Veneziani, M., and Vittorio, N., “Instrument, method, brightness, and polarization maps from the 2003 flight of BOOMERanG,” *A&A* **458**, 687–716 (Nov. 2006).
- [13] Pascale, E., Ade, P. A. R., Bock, J. J., Chapin, E. L., Chung, J., Devlin, M. J., Dicker, S., Griffin, M., Gundersen, J. O., Halpern, M., Hargrave, P. C., Hughes, D. H., Klein, J., MacTavish, C. J., Marsden, G., Martin, P. G., Martin, T. G., Mauskopf, P., Netterfield, C. B., Olmi, L., Patanchon, G., Rex, M., Scott, D.,

- Semisch, C., Thomas, N., Truch, M. D. P., Tucker, C., Tucker, G. S., Viero, M. P., and Wiebe, D. V., “The Balloon-borne Large Aperture Submillimeter Telescope: BLAST,” *ArXiv e-prints* **711** (Nov. 2007).
- [14] Yoon, K. W., Ade, P. A. R., Barkats, D., Battle, J. O., Bierman, E. M., Bock, J. J., Brevik, J. A., Chiang, H. C., Crites, A., Dowell, C. D., Duband, L., Griffin, G. S., Hivon, E. F., Holzappel, W. L., Hristov, V. V., Keating, B. G., Kovac, J. M., Kuo, C. L., Lange, A. E., Leitch, E. M., Mason, P. V., Nguyen, H. T., Ponthieu, N., Takahashi, Y. D., Renbarger, T., Weintraub, L. C., and Woolsey, D., “The Robinson Gravitational Wave Background Telescope (BICEP): a bolometric large angular scale CMB polarimeter,” in [*Millimeter and Submillimeter Detectors and Instrumentation for Astronomy III. Edited by Zmuidzin, Jonas; Holland, Wayne S.; Withington, Stafford; Duncan, William D. Proceedings of the SPIE, Volume 6275, pp. 62751K (2006).*], Presented at the Society of Photo-Optical Instrumentation Engineers (SPIE) Conference **6275** (July 2006).
- [15] Goldin, A., Bock, J. J., Hunt, C., Lange, A. E., LeDuc, H., Vayonakis, A., and Zmuidzin, J., “Samba: Superconducting antenna-coupled, multi-frequency, bolometric array,” *LOW TEMPERATURE DETECTORS: Ninth International Workshop on Low Temperature Detectors* **605**(1), 251–254, AIP (2002).
- [16] Vayonakis, A., Luo, C., Leduc, H. G., Schoelkopf, R., and Zmuidzin, J., “The millimeter-wave properties of superconducting microstrip lines,” *LOW TEMPERATURE DETECTORS: Ninth International Workshop on Low Temperature Detectors* **605**(1), 539–542, AIP (2002).
- [17] Hunt, C. L., Bock, J. J., Day, P. K., Goldin, A., Lange, A. E., LeDuc, H. G., Vayonakis, A., and Zmuidzin, J., “Transition-edge superconducting antenna-coupled bolometer,” in [*Millimeter and Submillimeter Detectors for Astronomy. Edited by Phillips, Thomas G.; Zmuidzin, Jonas. Proceedings of the SPIE, Volume 4855, pp. 318-321 (2003).*], Phillips, T. G. and Zmuidzin, J., eds., Presented at the Society of Photo-Optical Instrumentation Engineers (SPIE) Conference **4855**, 318–321 (Feb. 2003).
- [18] Irwin, K. D., “An application of electrothermal feedback for high resolution cryogenic particle detection,” *Applied Physics Letters* **66**, 1998–2000 (Apr. 1995).
- [19] Lee, A. T., Richards, P. L., Nam, S. W., Cabrera, B., and Irwin, K. D., “A superconducting bolometer with strong electrothermal feedback,” *Applied Physics Letters* **69**, 1801–1803 (Sept. 1996).
- [20] Gildemeister, J. M., Lee, A. T., and Richards, P. L., “A fully lithographed voltage-biased superconducting spiderweb bolometer,” *Applied Physics Letters* **74**, 868–+ (Feb. 1999).
- [21] Hunt, C. L., *Transition-edge superconducting antenna-coupled bolometer*, PhD thesis, California Institute of Technology, United States – California (Oct. 2004).
- [22] Battistelli, E. S., Amiri, M., Burger, B., Halpern, M., Knotek, S., Ellis, M., Gao, X., Kelly, D., Macintosh, M., Irwin, K., and Reintsema, C., “Functional Description of Read-out Electronics for Time-Domain Multiplexed Bolometers for Millimeter and Sub-millimeter Astronomy,” *Journal of Low Temperature Physics* **151**, 908–914 (May 2008).
- [23] Chervenak, J. A., Irwin, K. D., Grossman, E. N., Martinis, J. M., Reintsema, C. D., and Huber, M. E., “Superconducting multiplexer for arrays of transition edge sensors,” *Applied Physics Letters* **74**, 4043–+ (June 1999).
- [24] de Korte, P. A. J., Beyer, J., Deiker, S., Hilton, G. C., Irwin, K. D., Macintosh, M., Nam, S. W., Reintsema, C. D., Vale, L. R., and Huber, M. E., “Time-division superconducting quantum interference device multiplexer for transition-edge sensors,” *Review of Scientific Instruments* **74**, 3807–3815 (Aug. 2003).
- [25] Reintsema, C. D., Beyer, J., Nam, S. W., Deiker, S., Hilton, G. C., Irwin, K., Martinis, J., Ullom, J., Vale, L. R., and Macintosh, M., “Prototype system for superconducting quantum interference device multiplexing of large-format transition-edge sensor arrays,” *Review of Scientific Instruments* **74**, 4500–4508 (Oct. 2003).
- [26] Irwin, K. D., Audley, M. D., Beall, J. A., Beyer, J., Deiker, S., Doriese, W., Duncan, W., Hilton, G. C., Holland, W., Reintsema, C. D., Ullom, J. N., Vale, L. R., and Xu, Y., “In-focal-plane SQUID multiplexer,” *Nuclear Instruments and Methods in Physics Research A* **520**, 544–547 (Mar. 2004).
- [27] Holland, W., MacIntosh, M., Fairley, A., Kelly, D., Montgomery, D., Gostick, D., Atad-Ettedgui, E., Ellis, M., Robson, I., Hollister, M., Woodcraft, A., Ade, P., Walker, I., Irwin, K., Hilton, G., Duncan, W., Reintsema, C., Walton, A., Parkes, W., Dunare, C., Fich, M., Kycia, J., Halpern, M., Scott, D., Gibb, A., Molnar, J., Chapin, E., Bintley, D., Craig, S., Chylek, T., Jenness, T., Economou, F., and Davis, G., “SCUBA-2: a 10,000-pixel submillimeter camera for the James Clerk Maxwell Telescope,” in [*Millimeter*

and Submillimeter Detectors and Instrumentation for Astronomy III. Edited by Zmuidzinas, Jonas; Holland, Wayne S.; Withington, Stafford; Duncan, William D.. Proceedings of the SPIE, Volume 6275, pp. 62751E (2006).], Presented at the Society of Photo-Optical Instrumentation Engineers (SPIE) Conference **6275** (July 2006).

- [28] Fowler, J. W. and ACT Collaboration, “The Atacama Cosmology Telescope,” in [*Bulletin of the American Astronomical Society*], *Bulletin of the American Astronomical Society* **38**, 1227–+ (Dec. 2006).
- [29] Audley, M. D., Barker, R. W., Crane, M., Dace, R., Glowacka, D., Goldie, D. J., Lasenby, A. N., Stevenson, H. M., Tsaneva, V., Withington, S., Grimes, P., Johnson, B., Yassin, G., Piccirillo, L., Pisano, G., Duncan, W. D., Hilton, G. C., Irwin, K. D., Reintsema, C. D., and Halpern, M., “TES imaging array technology for C_IOVER,” in [*Millimeter and Submillimeter Detectors and Instrumentation for Astronomy III. Edited by Zmuidzinas, Jonas; Holland, Wayne S.; Withington, Stafford; Duncan, William D.. Proceedings of the SPIE, Volume 6275, pp. 627524 (2006).*], Presented at the Society of Photo-Optical Instrumentation Engineers (SPIE) Conference **6275** (July 2006).
- [30] Kovac, J. and BICEP/SPUD collaboration, “BICEP2 and SPUD: Searching for Inflation with Degree-Scale Polarimetry from the South Pole,” in [*Bulletin of the American Astronomical Society*], *Bulletin of the American Astronomical Society* **38**, 913–+ (Dec. 2006).
- [31] Chui, T. and et al. in preparation (2008).
- [32] Hu, W., Hedman, M. M., and Zaldarriaga, M., “Benchmark parameters for CMB polarization experiments,” *Phys. Rev. D* **67**, 043004–+ (Feb. 2003).
- [33] Rosset, C., Yurchenko, V. B., Delabrouille, J., Kaplan, J., Giraud-Héraud, Y., Lamarre, J.-M., and Murphy, J. A., “Beam mismatch effects in cosmic microwave background polarization measurements,” *A&A* **464**, 405–415 (Mar. 2007).
- [34] Jones, W. C., Montroy, T. E., Crill, B. P., Contaldi, C. R., Kisner, T. S., Lange, A. E., MacTavish, C. J., Netterfield, C. B., and Ruhl, J. E., “Instrumental and analytic methods for bolometric polarimetry,” *A&A* **470**, 771–785 (Aug. 2007).